

# Probing the density dependence of the symmetry potential in intermediate energy heavy ion collisions

Qingfeng Li<sup>1,\*</sup>, Zhuxia Li<sup>1,2</sup>, Sven Soff<sup>3</sup>,  
 Raj K. Gupta<sup>1,4†</sup>, Marcus Bleicher<sup>3</sup>, and Horst Stöcker<sup>1,3</sup>

1) *Frankfurt Institute for Advanced Studies (FIAS),*

*Johann Wolfgang Goethe-Universität, Max-von-Laue-Str. 1,*

*D-60438 Frankfurt am Main, Germany*

2) *China Institute of Atomic Energy,*

*P.O. Box 275 (18), Beijing 102413, P.R. China*

3) *Institut für Theoretische Physik,*

*Johann Wolfgang Goethe-Universität, Max-von-Laue-Str. 1,*

*D-60438 Frankfurt am Main, Germany*

4) *Department of Physics, Panjab University, Chandigarh – 160014, India.*

## Abstract

Based on the ultrarelativistic quantum molecular dynamics (UrQMD) model, the effects of the density-dependent symmetry potential for baryons and of the Coulomb potential for produced mesons are investigated for neutron-rich heavy ion collisions at intermediate energies. The calculated results of the  $\Delta^-/\Delta^{++}$  and  $\pi^-/\pi^+$  production ratios show a clear beam-energy dependence on the density-dependent symmetry potential, which is stronger for the  $\pi^-/\pi^+$  ratio close to the pion production threshold. The Coulomb potential of the mesons changes the transverse momentum distribution of the  $\pi^-/\pi^+$  ratio significantly, though it alters only slightly the  $\pi^-$  and  $\pi^+$  total yields. The  $\pi^-$  yields, especially at midrapidity or at low transverse momenta and the  $\pi^-/\pi^+$  ratios at low transverse momenta, are shown to be sensitive probes of the density-dependent symmetry potential in dense nuclear matter. The effect of the density-dependent symmetry potential on the production of both,  $K^0$  and  $K^+$  mesons, is also investigated.

PACS numbers: 24.10.Lx, 25.75.Dw, 25.75.-q

---

\* Fellow of the Alexander von Humboldt Foundation.

† DFG Mercator Guest Professor.

## I. INTRODUCTION

The study of isospin effects in nuclear matter or finite nuclei is a well established topic in nuclear physics, as well as in nuclear astrophysics [1, 2]. On the mean field level, this means the contribution of the symmetry energy of particles to the total energy (see, e.g., the recent Refs. [3, 4, 5, 6, 7, 8, 9, 10]), and on the two-body collision level, detailed experimental data on the free proton-proton and neutron-proton scattering cross sections have been obtained [11] as a function of energy ranging from the Coulomb barrier to ultra high energy interactions. At low energies (up to several hundreds of MeV/nucleon), large differences are visible between the proton-proton and the neutron-proton cross sections. In heavy ion collisions (HICs), it is also necessary to study the effect of density on the isospin-dependent nucleon-nucleon cross sections.

Recently, we have explored the density- and temperature-dependence of the nucleon-nucleon elastic scattering cross sections in collisions between neutron-rich nuclei at intermediate energies [12]. We found a density dependence of the elastic scattering cross sections. This work is based on the theory of quantum hydrodynamics (QHD), in which the interaction between nucleons is described by the exchange of  $\sigma$ ,  $\omega$ ,  $\rho$ , and  $\delta$  mesons. Since, in the QHD theory, both the mean field and the collision term originate from the same Lagrangian density, the density-dependence of the symmetry energy is our next subject to investigate. Currently the exploration of the isospin dependence of the nuclear interaction (especially in exotic and very isospin-asymmetric systems) has gained high interest [4, 5, 6, 7, 9, 13, 14]. In particular, the density dependence of the symmetry energy in *dense* nuclear matter has to be studied in detail, because it suffers from large uncertainties in the predictions of various theoretical models [15, 16]. Based on the QHD theory, with a similar effective Lagrangian density [6, 17, 18], the main uncertainty of the density dependence of the symmetry energy results from the uncertainties of the density-dependent coupling strengths of various meson-baryon interactions, especially that of  $\rho - N$  and  $\delta - N$  interactions [6]. Also, in forthcoming experiments at the Rare Isotope Accelerator (RIA) laboratory (USA) and at the new international accelerator facility FAIR (Facility for Antiproton and Ion Research) at the Gesellschaft für Schwerionenforschung (GSI, Germany), more neutron-rich beams are planned to be adopted, and hence call for further theoretical studies on isospin-dependent HICs in the intermediate energy region.

In order to obtain detailed information on the density dependence of the symmetry energy in dense nuclear matter, quite a few sensitive probes were brought up for experiments in recent years: e.g., the  $\pi^-/\pi^+$  yield ratio, the pion flow, the transverse momentum distribution of  $\pi^-/\pi^+$  ratios, the neutron-proton differential flow [4], and the isospin equilibration and stopping [7, 19, 20]. More recently, we have also investigated [9] the sensitivity of the  $\Sigma^-/\Sigma^+$  ratio on the density-dependent symmetry potentials. Further investigations seem to be worthwhile to shed light on the rather unclear isospin-independent and -dependent mean-field potentials of the hyperons. Since the contribution of the symmetry energy to the whole dynamics of HICs is rather small at SchwerIonen Synchrotron (SIS) energies, it is all the more difficult to explore the density dependence of the symmetry energy based on the current experimental situation. Hence, in theory, more sensitive probes should be searched for.

Also, such a detailed analysis is quite necessary and important because of the following arising questions: Is the effect of the density-dependent symmetry energy on the  $\pi^-/\pi^+$  ratio influenced by the beam energy? In which momentum, rapidity, or phase-space, region are the pion yields more suitable to probe the density-dependent symmetry energy? And, how does the Coulomb potential of mesons affect the emission of pions? Gaitanos *et al.* [6, 7] found that for beam energies higher than about  $2A$  GeV, the sensitivity of the  $\pi^-/\pi^+$  ratio to the form of the symmetry energy at high densities is strongly reduced. Furthermore, they found that the  $\pi^-/\pi^+$  ratio at high transverse momenta  $p_t$  could offer sound information on the density dependence of the symmetry energy. B.-A. Li *et al.* [5] revisited the  $\pi^-/\pi^+$  ratio by using an up-dated, new version of the isospin-dependent Boltzmann-Uehling-Uhlenbeck (IBUU04) model, in which an isospin- and momentum-dependent single nucleon potential was adopted. They found that the sensitivity of the  $\pi^-/\pi^+$  ratio on the density-dependence of the symmetry energy becomes obvious after considering the momentum-dependent single nucleon potential. They also noticed the effect of the Coulomb potential on the  $\pi$  production, especially on the transverse momentum spectra. Their work implied that it is sufficient to measure accurately the low-energy (or the low-transverse-momentum  $p_t$ ) pions, instead of the whole spectrum. In this paper, we address these aspects of the problem on the basis of the ultrarelativistic quantum molecular dynamics (UrQMD) model.

In this work, we also investigate the  $K^0/K^+$  production ratio as a probe of the density-dependent symmetry potential in dense nuclear matter. Based on the constituent quark

picture the  $K^0$  meson contains one  $d$ -quark while the  $K^+$  contains one  $u$ -quark, as well as one  $\bar{s}$ -quark in each meson. This is closely related to the isospin asymmetry of the nuclear medium at SIS energies. Furthermore, experimentally, the effects of system parameters, such as beam energy or impact parameter, on the sensitive probes also have to be kept in mind. Theoretically, the uncertainty of the isospin-independent nuclear equation of state (EoS), as well as the contribution of the Coulomb potential of mesons, might alter the calculated results of these probes, hence, they could even modify the conclusions and should be checked carefully.

In the UrQMD model (version 1.3) [20, 21, 22, 23], adopted here, we find that most of the calculations can simultaneously reproduce many experimental measurements, which offers a good starting point for studying the isospin effects at SIS energies. In this work, a 'hard' and a 'soft' Skyrme-type EoS, without momentum dependence, are adopted for central ( $b = 0 - 2$  fm) or near-peripheral ( $b = 5 - 8$  fm)  $^{132}Sn + ^{132}Sn$  reactions at beam energies  $E_b = 0.5A$  and  $1.5A$  GeV. We consider phenomenological density-dependent symmetry potentials, which will be discussed in more detail in the next section. The Coulomb potentials of the mesons are switched on or off in order to analyze more conveniently the contributions of the various symmetry potentials to the dynamical evolution of the hadrons in the nuclear medium.

The paper is arranged as follows: In Section II, we clarify the inclusion of the isospin-dependent part of the mean field in the UrQMD transport model. In Section III, some basic isospin effects on the dynamics of the baryons (here the nucleons and  $\Delta(1232)$ ) in SIS energy HICs are shown. In Section IV, firstly the effects of the isospin-independent EoS, the beam energy, and the impact parameter on the emitted pion yields and the  $\pi^-/\pi^+$  production ratios are discussed. Then, the various phase-space distributions of pion yields and the  $\pi^-/\pi^+$  ratios, with the different density dependences of the symmetry potentials, are investigated. At the end of this section, the sensitivity of the  $K^0/K^+$  ratio to the density dependence of the symmetry potential is discussed. Finally, the conclusions and outlook are given in Section V.

## II. THE TREATMENT OF THE POTENTIAL UPDATE OF HADRONS IN THE URQMD MODEL

The initialization of neutrons and protons, the corresponding Pauli blocking, the Coulomb potential of baryons, and the isospin dependence of the nucleon-nucleon cross sections have been introduced explicitly in the standard UrQMD model. In order to study the isospin effects in intermediate energy HICs, it is required to further introduce the symmetry potential of baryons.

The isospin-dependent EoS for asymmetric nuclear matter can be expressed as (see, *e.g.*, [24])

$$e(u, \delta) = \frac{\epsilon(u, \delta)}{\rho} = e_0(u) + e_{\text{sym}}(u)\delta^2, \quad (1)$$

where  $u = \rho/\rho_0$  is the reduced nuclear density and  $\delta = (\rho_n - \rho_p)/\rho$  is the isospin asymmetry in terms of neutron ( $\rho_n$ ) and proton ( $\rho_p$ ) densities. The  $e_0(u)$  term is the isospin-independent part, which includes the Skyrme and the Yukawa potentials in the UrQMD model [20]. The Yukawa parameter is related to the Skyrme parameters since in infinite nuclear matter the contribution of the Yukawa potential to the total energy acts like a two-body Skyrme contribution. For comparison, both a soft ( $K = 200$  MeV) and a hard ( $K = 300$  MeV, the default parametrization in this work) EoS are adopted in this work.  $e_{\text{sym}}$  is the symmetry energy per nucleon, in which the kinetic ( $v_{\text{sym}}^{\text{kin}}$ ) and potential ( $v_{\text{sym}}^{\text{pot}}$ ) contributions are included. The average symmetry potential energy can be expressed as

$$v_{\text{sym}}^{\text{pot}} = e_a F(u), \quad (2)$$

where  $e_a$  is the symmetry-potential strength and  $F(u)$  is the density-dependent part. If the Fermi-gas model is adopted, the symmetry-potential strength  $e_a$  is related to the symmetry energy at normal density,  $S_0$ , by

$$S_0 \simeq e_a + \frac{\epsilon_F}{3}. \quad (3)$$

Here,  $\epsilon_F$  is the Fermi kinetic energy at normal nuclear density.

The relativistic mean field calculations [6] show a small variation of the symmetry kinetic energy extracted from various models, and the uncertainty of the symmetry energy with nuclear density results mainly from the symmetry potential energy. Concerning the symmetry potential energy, both the symmetry energy coefficient  $S_0$  and the density dependence of the symmetry energy are quite uncertain. For  $S_0$ , deduced from the isovector GDR in  $^{208}Pb$  and

from the available data of differences between neutron and proton radii for  $^{208}Pb$  and several  $Sn$  isotopes, a rather small range of values is  $32 \text{ MeV} \leq S_0 \leq 36 \text{ MeV}$  [25]. More recently, a new value of  $S_0 \simeq 31 \text{ MeV}$  was obtained, based on the consistent folding analysis of the  $p(^6He, ^6He)p$  elastic scattering and  $p(^6He, ^6Li^*)n$  charge exchange reaction data measured at  $E_{\text{Lab}} = 41.6 \text{ MeV}$  [26], while  $S_0 = 34 \text{ MeV}$  was obtained in a calculation made within the relativistic Brueckner framework, using the Bonn A potential [27]. Thus, it is necessary to further investigate the uncertainty of the  $S_0$  value [28]. In this paper, however, the value  $S_0 = 34 \text{ MeV}$  is adopted, since we endeavor to investigate the density dependence of the symmetry potential energy.

In order to mimic the strong density dependence of the symmetry potential at high densities, we adopt the form of  $F(u)$ , used in [4], as

$$F(u) = \begin{cases} F_1 = u^\gamma & \gamma > 0 \\ F_2 = u \cdot \frac{a-u}{a-1} & a > 1 \end{cases} . \quad (4)$$

Here,  $\gamma$  is the strength of the density dependence of the symmetry potential. We choose  $\gamma = 0.5$  and  $1.5$ , denoted as the symmetry potentials F05 and F15, respectively.  $a$  (in  $F_2$ ) is the reduced critical density; for  $u > a$ , the symmetry potential energy is negative. We adopt  $a = 3$  in this paper and the respective symmetry potential is named as Fa3. The symmetry potentials F05, F15, and Fa3 are shown in Fig. 1 as a function of the reduced nuclear density  $u$ , compared with a linear density-dependent symmetry potential.

From Fig. 1, it is apparent that for  $u < 1$ , F05>Fa3>F15, whereas for  $u > 1$ , F15>F05>Fa3. F05 is larger than Fa3 for all densities. This means that for neutron-rich HICs at intermediate energies, less neutrons are pushed into the low density region ( $u < 1$ ) as well as into the high density region ( $u > 1$ ) for density dependence Fa3, as compared to F05. In other words, the symmetry-potential parametrization F05 is always stiffer than Fa3 (at both subnormal and higher densities), except at normal nuclear density.

Besides nucleons (N), the resonances  $N^*(1440)$ ,  $\Delta(1232)$ , and the hyperons  $\Lambda$  and  $\Sigma$  should be considered for SIS energy HICs, where the  $\Delta(1232)$  is dominating, denoted as  $\Delta$  in short. For simplicity, the isospin-independent part of the EoS,  $e_0(u)$ , for all other baryons is taken to be the same as for the nucleons. The symmetry potentials for the resonances are obtained through the constants of isospin coupling (the Clebsch-Gordan coefficients) in the process of  $\Delta$  [or  $N^*(1440)$ ]  $\leftrightarrow \pi N$ . For hyperons, based on the analysis of the Lane potential [29, 30], we simply take the symmetry potential of hyperons to be nucleon-like.

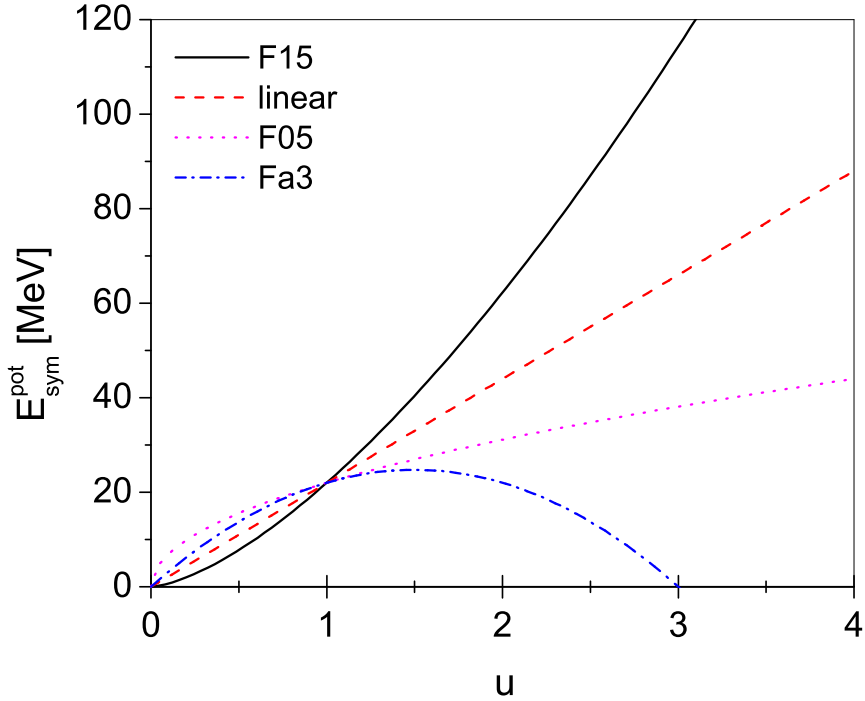


FIG. 1: The symmetry potential energy of nucleons as a function of the reduced nuclear density  $u$ , using various density dependences (see text).

However, the symmetry potential of excited states of hyperons is not considered, for lack of information.

Combining both, resonances and hyperons, we express the symmetry potential in a unified form, which reads as

$$v_{\text{sym}}^B = \alpha v_{\text{sym}}^n + \beta v_{\text{sym}}^p, \quad (5)$$

where the values of  $\alpha$  and  $\beta$  for different baryons (B) are listed in Table I. From this table we can see that the symmetry potentials of  $\Delta^-$  and  $\Sigma^-$  are neutron-like and those of  $\Delta^{++}$  and  $\Sigma^+$  are proton-like. On the other hand, the symmetry potentials of  $\Delta^0$ ,  $\Delta^+$ ,  $N^*(1440)$ ,  $\Sigma^0$ , and  $\Lambda$  are a mixture of the neutron and proton symmetry potentials.

In the standard UrQMD model (version 1.3), the cascade mode is usually adopted for produced mesons. In order to investigate the phase-space distributions of pions, especially the transverse momentum distributions in intermediate energy HICs, the Coulomb potential

TABLE I: Values  $\alpha$  and  $\beta$  for the symmetry potentials (Eq. 5) of different nucleon and  $\Delta$  resonances, as well as hyperons.

B	$\alpha$	$\beta$	B	$\alpha$	$\beta$
$N^{*0}(1440)$	1/3	2/3	$\Lambda$	1/2	1/2
$N^{*+}(1440)$	2/3	1/3	$\Delta^-$	1	0
$\Sigma^-$	1	0	$\Delta^0$	2/3	1/3
$\Sigma^0$	1/2	1/2	$\Delta^+$	1/3	2/3
$\Sigma^+$	0	1	$\Delta^{++}$	0	1

of mesons should be considered explicitly [5, 6, 31]. Thus, in this paper, we also investigate the contribution of the Coulomb potentials between mesons and baryons. Other mean-field potentials of mesons are not yet considered.

### III. EFFECTS OF THE SYMMETRY POTENTIAL ON THE DYNAMICS OF NUCLEONS AND $\Delta$ 'S

First of all, let us discuss the basic consequences of the density dependence of the symmetry potentials in neutron-rich HICs at SIS energies. Fig. 2 (top) shows the time evolution of the neutron and proton numbers for the symmetry potentials F15, F05, and Fa3. Here, we do not distinguish whether the nucleons are free or bound in heavier fragments. The beam energies are  $E_b = 0.5A$  and  $1.5A$  GeV and central collisions ( $b = 0 - 2$  fm) are chosen. From this plot, we notice that independent of the choice of the density dependence of the symmetry potential, the neutron numbers reach their minima at  $\sim 15$  fm/ $c$  and  $10$  fm/ $c$ , for the beam energies  $E_b = 0.5A$  and  $1.5A$  GeV, respectively. At this time the central nuclear density reaches its maximum and some of the neutrons are excited (to  $N^*$  or  $\Delta$ ) or converted to other baryons (e.g., hyperons) through various baryon-baryon or meson-baryon collisions. We also notice that the higher the beam energy, the more excited baryon states are produced. There are obviously less excited protons than neutrons at the compression stage. In other words, at the compression stage, the effect on the neutron number is stronger than on the proton number, which is due to the neutron-rich nuclear environment. After the decay of these unstable baryons, the emitted mesons (especially, the pions) alter the neutron/proton

ratio (the neutron number decreases, and, correspondingly, the proton number increases), and hence the ratio tends to become unity with an increase of the beam energy. In addition the effect of the density-dependent symmetry potentials on the dynamical process is smaller at higher energies [9]. With a softer symmetry potential Fa3, more neutrons are excited at the compression stage, which is clearly due to more neutrons being kept by the softer symmetry potential in the high density region, as implied from Fig. 1.

In Fig. 2 (bottom), the neutron/proton ratio of the all (free and bound) nucleons at freeze-out time ( $t_f = 50 \text{ fm}/c$ , the maximum time used in the top plot) is shown as a function of the normalized rapidity ( $y_c^{(0)} = y_c/y_{\text{beam}}$ , where  $y_c$  is the rapidity of the particle in the center-of-mass system and  $y_{\text{beam}}$  is the beam rapidity). At  $E_b = 0.5A \text{ GeV}$ , the density dependence of the symmetry potential influences the neutron/proton ratio strongly, whereas at  $E_b = 1.5A \text{ GeV}$  the sensitivity is reduced, especially at midrapidity. This happens not only due to the relatively weak effect of the EoS, as compared to the two-body collision dynamics, but also due to the nucleon-nucleon cross sections at higher energies that depend less on isospin. Secondly, in the projectile and target rapidity regions, the  $n/p$  ratio is more sensitive to the density dependence of the symmetry potential as compared to the midrapidity region. Less collisions take place in the projectile and target rapidity regions than in the midrapidity region (see also, Fig. 3). Thirdly, the  $n/p$  ratio is larger with a softer symmetry potential Fa3 than that with F15, and vice versa in the projectile-target regions. The nucleons in the midrapidity region represent mainly the behavior of symmetry potential at high densities, where more neutrons are kept with a soft symmetry potential. We should also notice that at midrapidity, the difference of the ratios with the F05 and Fa3 symmetry potentials is almost negligible. From Fig. 1 we can see that F05 is always stiffer than Fa3 at both low and high densities, thus the  $n/p$  ratio is also influenced by the density dependence of the symmetry potential at subnormal densities. Therefore, in order to investigate any isospin dependences, it is very important to know the correct density-dependent form of the symmetry potential at *both*, low and high densities.

Fig. 3 shows the calculated rapidity distribution of the collision number of neutrons and protons (upper plot), and the corresponding ratios (lower plot). Evidently, at both energies, the collision number of nucleons has a strong maximum at midrapidity. The collision number increases with beam energy, especially for neutrons because of the neutron-rich system. The average proton collision number is always larger than the average neutron collision number

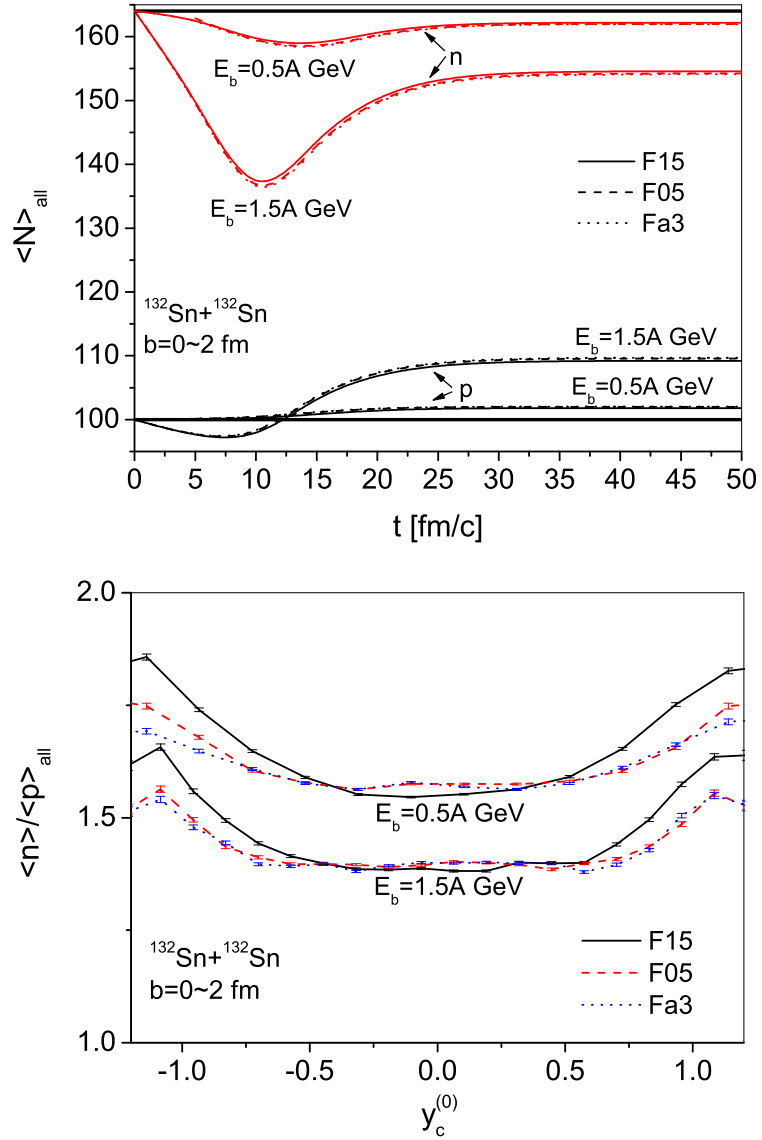


FIG. 2: Top: Time evolution of the neutron and proton numbers for central  $^{132}\text{Sn} + ^{132}\text{Sn}$  collisions at beam energies  $0.5A$  and  $1.5A$  GeV. For the "hard" EoS, three different forms of the symmetry potential are used (see text). The two horizontal solid (thick) lines represent the initial neutron and proton numbers of the system. Bottom: normalized rapidity distribution of the neutron/proton ratio of all nucleons at freeze-out time (see text). The error bars show the statistical error.

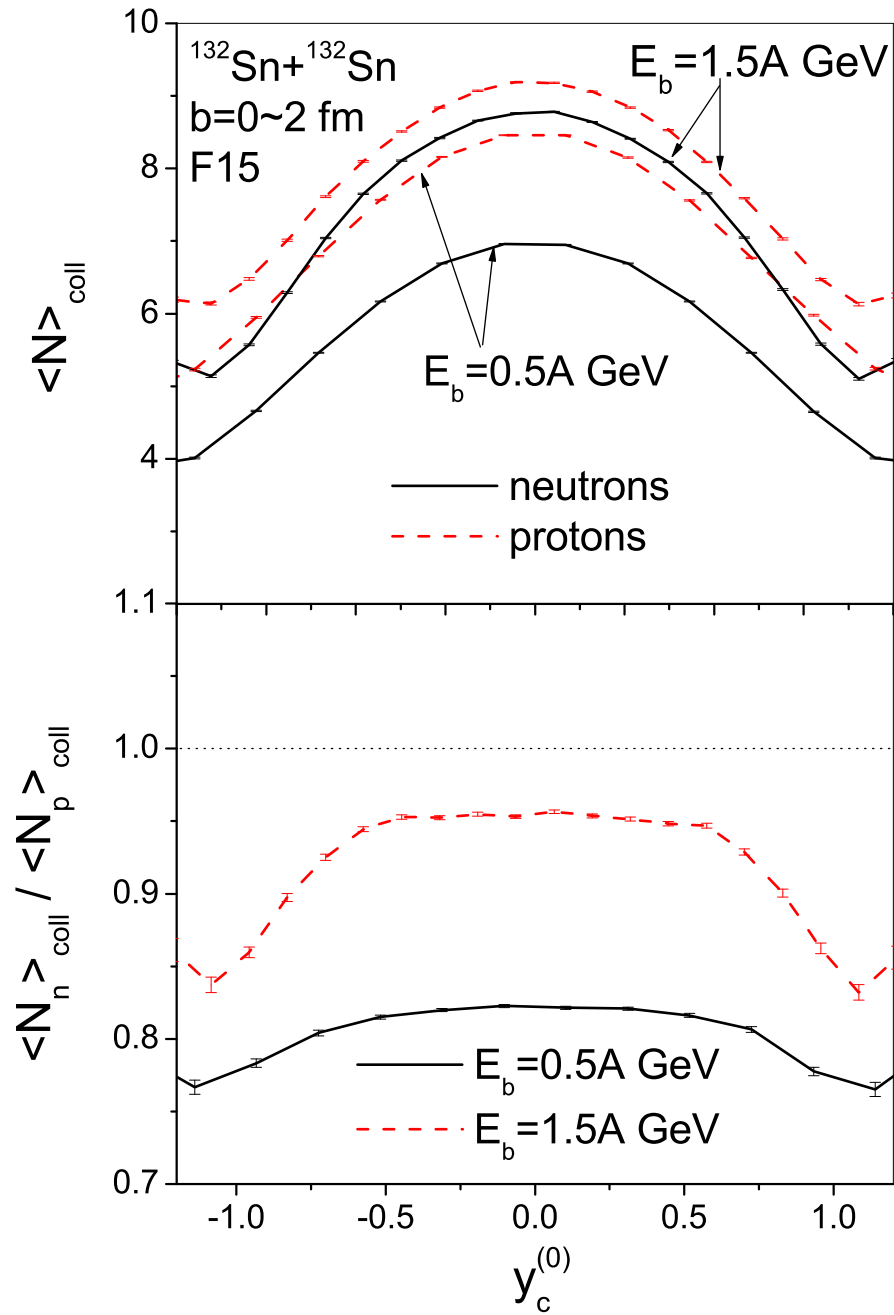


FIG. 3: Top: Normalized rapidity distributions of the collision number of neutrons and protons at energies  $E_b = 0.5A$  and  $1.5A$  GeV. The case of the symmetry potential F15 is shown. Bottom: The corresponding ratios between the collision numbers of neutrons and protons.

because of the differences in the nucleon-nucleon cross sections at intermediate energies [11]. When the beam energy increases from  $0.5A$  to  $1.5A$  GeV, this isospin effect of the nucleon-nucleon cross section is largely reduced, so that the ratio between the neutron and proton collision numbers approach unity, which is shown in the lower part of Fig. 3. In the midrapidity region, the collision ratio of neutrons and protons is  $\sim 82\%$  at  $E_b = 0.5A$  GeV, which increases to  $\sim 95\%$  at  $E_b = 1.5A$  GeV.

Since, in the SIS energy region,  $\pi$ -mesons are mainly produced from decaying  $\Delta$ 's, it is also important to investigate the dynamics of the  $\Delta$ 's with respect to the symmetry potential. Fig. 4 shows the time evolution of the various components of  $\Delta$  (upper plot) and the ratio  $\Delta^-/\Delta^{++}$  (lower plot) for the symmetry potentials F15 and Fa3 and for central  $^{132}\text{Sn}+^{132}\text{Sn}$  collisions at the two energies  $E_b = 0.5A$  and  $1.5A$  GeV. In the upper plot, only the case  $E_b = 0.5A$  GeV is shown since, at  $E_b = 1.5A$  GeV, the effect of the density dependence of the symmetry potentials on the  $\Delta$  production is almost negligible. This is supported by the time evolution of the ratio  $\Delta^-/\Delta^{++}$  at  $E_b = 1.5A$  GeV in the lower plot.

From the upper part of Fig. 4, it is clear that the effect of the density-dependent symmetry potentials on the time evolution is strongest for the  $\Delta^-$  production, like for neutrons in Fig. 2. From the time evolution of the  $\Delta^-/\Delta^{++}$  ratio in the lower plot of Fig. 4, we further notice that, similar to the case of nucleons, the effect of the density-dependent symmetry potentials on the  $\Delta^-/\Delta^{++}$  ratio is largely reduced at the higher beam energy  $1.5A$  GeV. And the time evolution of this ratio is nearly flat since, at this energy, the effect of the Coulomb and the symmetry potentials becomes small. At the lower beam energy  $0.5A$  GeV and during the compression stage ( $t \lesssim 12 \text{ fm}/c$ ), the  $\Delta^-/\Delta^{++}$  ratio decreases with time while it increases at the later stage, the expansion stage. This is apparently due to the dynamically mutual interaction between the Coulomb and the symmetry potentials: along the time evolution at the compression stage, more neutrons are pushed out because the relative strength of the symmetry potential as compared to the Coulomb potential increases. This can be understood from the study on the ratio of preequilibrium neutron number to proton number in the intermediate-energy neutron-rich HICs in Ref. [32]: this ratio is larger than the initial neutron/proton ratio of the colliding system; at the expansion stage, more protons are pushed out due to the stronger Coulomb potential as compared to the symmetry potential. Note that the increase of the  $\Delta^-/\Delta^{++}$  ratio at the late stage is stronger for the symmetry potential Fa3 than for F15. The time evolution of the  $\Delta$  abundancies, depending

on the symmetry potential, should also affect the production of pions.

Besides the  $\pi$ -yields, the pion spectra should also be influenced by the decay of  $\Delta$ 's. Fig. 5 shows the transverse momentum spectrum of  $\Delta$ 's (upper plot) and the  $\Delta^-/\Delta^{++}$  ratios (lower plot) at  $t = 20$  fm/ $c$  and  $E_b = 0.5A$  GeV, for the symmetry potentials F15, F05, and Fa3. We notice from the upper part of Fig. 5 that, similar to the neutrons in Fig. 2, the effect of different density-dependent symmetry potentials is strongest for the  $\Delta^-$ . From the lower plot of Fig. 5 we can see that, at lower  $p_t^{\text{cm}}$  ( $p_t^{\text{cm}} \lesssim 0.8$  GeV/ $c$ ), the  $\Delta^-/\Delta^{++}$  ratios are quite different for the symmetry potentials F15 and F05 (or Fa3), and the results of the F05 and Fa3 symmetry potentials are nearly the same. These results are similar to the rapidity distribution of the neutron/proton ratio, shown in Fig. 2.  $\Delta$ 's with low transverse momenta are not produced from very high densities, namely around normal density, where the difference between F05 and Fa3 is quite small and the effect of F05 and Fa3 on the  $\Delta^-/\Delta^{++}$  ratio are cancelled strongly between low and high densities. For  $p_t^{\text{cm}} \gtrsim 0.8$  GeV/ $c$ , the differences between the results of F05 and Fa3 become distinguishable because  $\Delta$ 's with the high transverse momenta are mainly produced from the central high-density region. Thus the  $\Delta^-/\Delta^{++}$  ratio at high transverse momenta can provide clearer information on the density dependence of the symmetry potential. In the next section, we investigate the question to what extent this property could be transferred to  $\pi$ 's, especially when the contribution of the Coulomb potential of mesons is also considered.

#### IV. EFFECTS OF THE SYMMETRY POTENTIAL ON THE $\pi$ AND $K$ PRODUCTION

Fig. 6 shows the time evolution of the  $\pi$  abundancies (upper plot) and their ratios (lower plot) for the density-dependent symmetry potentials F15, F05, and Fa3. Here, the Coulomb potential of mesons is switched off. However, for comparison, we also provide the results (for the case of F05 and at  $E_b = 0.5A$  GeV) when the Coulomb potential of mesons is taken into account (solid points in Fig. 6 at time  $t = 45$  fm/ $c$ ). Apparently, the effect of the Coulomb potential of mesons on the  $\pi$ -yields is quite small. We also find that the effect of the different symmetry potentials on the  $\pi^-/\pi^+$  ratio is hardly affected by the Coulomb potential of mesons although it alters the absolute value of the ratio. The number of  $\pi^-$  grows much stronger than the number of  $\pi^+$ , almost independent of the choice of the

symmetry potentials F05 and Fa3. The  $\pi^-$ -yields are, however, smaller for F15. So is the  $\pi^-/\pi^+$  ratio at  $E_b = 0.5A$  GeV. On the other hand, for the higher beam energy  $E_b = 1.5A$  GeV, the ratios are almost independent of the symmetry potentials. (These results are clearly due to the properties of  $\Delta$ 's, shown in Figs. 4 and 5). Therefore, it is necessary to pay attention to the energy dependence of the isospin effect on the  $\pi^-/\pi^+$  ratios as well.

Next, we show the dependence of the  $\pi^-/\pi^+$  ratio on various isospin-independent EoS and impact parameter  $b$ . In view of the above noted beam-energy dependence, we only consider the lower beam energy  $E_b = 0.5A$  GeV in the following. Fig. 7 shows the results for two EoS and two centralities. The effect of the density-dependent symmetry potentials on the  $\pi^-/\pi^+$  ratios is almost not affected by the uncertainty of the isospin-independent EoS. That is, the absolute shift in the  $\pi^-/\pi^+$  ratio due to different symmetry potentials remains almost the same, independent of the stiffness of the isospin-independent EoS. On the other hand, at larger impact parameters ( $b = 5 \sim 8$  fm), the  $\pi^-/\pi^+$  ratio is even more sensitive to the density dependence of the symmetry potential.

The rapidity  $y_c$  and the polar angle  $\theta_c$  (in the center-of-mass system) distributions of  $\pi^-$  and  $\pi^+$  for various density-dependent symmetry potentials are shown in Fig. 8. The influence of the density-dependent symmetry potentials on the  $\pi$ -multiplicity distributions is strongest at midrapidity and at polar angles around  $90^\circ$ . This holds in particular for the  $\pi^-$  distribution, which was also seen in [5] for the kinetic energy spectrum of pions in central  $^{132}\text{Sn} + ^{124}\text{Sn}$  reactions at  $E_b = 0.4A$  GeV.

The upper two plots of Fig. 9 show the transverse momentum distributions of  $\pi^-$  and  $\pi^+$ , with and without the contribution of the Coulomb potentials of mesons, as well as with a rapidity-cut ( $|y_c| < 0.2$ ) (left plots) and without any kinematical cut (right plots), for the symmetry potential F05. This is important because, in recent years, several experiments on charged pion production at intermediate energies were performed by the FOPI Collaboration at GSI where the possible contribution of the Coulomb potentials of pions to the  $\pi$ -transverse momentum distribution was also discussed [31, 33]. Although, as shown in Fig. 6, the effect of the Coulomb potential of mesons on the total  $\pi$  yield is small, Fig. 9 demonstrates that it strongly influences the momentum distribution; the Coulomb potential of mesons always shifts the  $\pi^-$  to lower, and the  $\pi^+$  to higher  $p_t^{\text{cm}}$  for the neutron-rich systems, in line with Ref. [5]. With the rapidity-cut  $|y_c| < 0.2$ , this effect becomes even more pronounced; as a result, the transverse momentum distribution of the  $\pi^-/\pi^+$  ratio at low  $p_t^{\text{cm}}$  becomes steeper

than the one without the rapidity cut (lower plots in Fig. 9 show the corresponding  $\pi^-/\pi^+$  ratios for the symmetry potentials F15, F05, and Fa3). If the Coulomb potential of mesons is switched off, the  $\pi^-/\pi^+$  ratio without rapidity-cut is nearly constant at low transverse momenta ( $p_t^{\text{cm}} < 0.3 \text{ GeV}/c$ ). With the rapidity-cut ( $|y_c| < 0.2$ ) it increases weakly with  $p_t^{\text{cm}}$  because of the contribution of the Coulomb potential of  $\Delta$ 's. At higher transverse momenta ( $p_t > 0.4 \text{ GeV}/c$ ), and with rapidity-cut (lower-left plot of Fig. 9), the effect of the density-dependent symmetry potentials on the  $\pi^-/\pi^+$  ratios is noticeable; the difference is also obvious for F05 and Fa3. It is recalled that a similar phenomenon can be seen in Fig. 5 for the  $\Delta^-/\Delta^{++}$  ratios. However, when the Coulomb potentials of mesons are taken into account, the effect of the density-dependent symmetry potentials on the  $\pi^-/\pi^+$  ratios at high transverse momenta is largely reduced, regardless of a rapidity cut. It was pointed out in [5] that the Coulomb potential is stronger than the symmetry potential, and the Coulomb potential acts directly on the charged pions but the symmetry potential does not, such that the  $\pi$ 's emitted from the dense region, which have higher  $p_t^{\text{cm}}$ , may be influenced much more by their Coulomb potential than by the symmetry potential. Considering the limit of experiments so far, we claim that the  $\pi^-/\pi^+$  production ratio at  $p_t^{\text{cm}} = 0.1 \text{ GeV}/c$  is a suitable candidate for probing the density dependence of the symmetry potential, which is discussed in more detail in [34].

Fig. 10 shows the density distribution of pion emission, with and without Coulomb potential of mesons. In the upper plot, the percentages of each component of  $\pi$  and of the total  $\pi$  yield are shown as a function of the reduced density  $u$ , in steps of  $\Delta u = 0.2$ , with the Coulomb potential of mesons included. Most pions are emitted from densities higher than normal nuclear density (especially from the density region  $u \sim 1 - 2$ ); a few pions ( $\sim 16\%$ ) are emitted from subnormal densities. This follows from Fig. 5 where quite a few  $\Delta$ 's are transported close to normal nuclear density. As these  $\Delta$ 's decay, some of them also appear at subnormal densities.

In the lower part of Fig. 10, the ratios of the percentages of  $\pi^-$  and  $\pi^+$  are shown as a function of the reduced density  $u$ , with and without the Coulomb potential of mesons. The ratios are always larger at lower densities than at higher densities since at the late stage, where the nuclear density decreases, the  $\Delta^-/\Delta^{++}$  ratio (shown in Fig. 4) increases with time. When the Coulomb potential of mesons is taken into account, more  $\pi^-$  mesons are decelerated because of the larger amount of the negatively charged particles in the low

density region, and are thus emitted with low momenta which leads to the rise of the  $\pi^-/\pi^+$  ratios at low  $p_t^{\text{cm}}$ , as shown in Fig. 9.

Besides the  $\pi^-/\pi^+$  ratios, the  $K^0/K^+$  ratios are also thought to be a suitable candidate to probe the density dependence of the symmetry potential in dense nuclear matter, as already discussed in the Introduction. Fig. 11 shows the time evolution of the  $K^0$  and  $K^+$  abundancies, as well as their ratios  $K^0/K^+$ , for central  $^{132}\text{Sn} + ^{132}\text{Sn}$  collisions at beam energy  $1.5A$  GeV and for the symmetry potentials F15 and Fa3. Similar to the  $\pi$  production, the effect of different density dependences of the symmetry potential on the kaon yields is quite reduced at higher energies.

In SIS energy HICs, kaons are emitted mainly from the high density region and at the early stage of the reaction. The dominant production channels are  $BB \rightarrow BB^* \rightarrow BKY$  and  $B\pi \rightarrow B^* \rightarrow KY$  (here  $Y$  represents a hyperon). With a softer symmetry potential, in the neutron-rich nuclear medium, more neutrons (protons) are shifted to the high (low) density region and hence more negatively (less positively) charged  $B^*$  are produced, and the  $K^0/K^+$  ratio increases. Thinking of the energy dependence, the kaon production at energies much lower than its threshold ( $\sim 1.58$  GeV from the nucleon-nucleon interaction in free space) might be more sensitive to the density dependence of the symmetry potential. As an example, we have also calculated the kaon yields from the reaction  $^{208}\text{Pb} + ^{208}\text{Pb}$  at  $E_b = 0.8A$  GeV and  $b = 7 \sim 9$  fm with the symmetry potentials F15 and Fa3: the  $K^0/K^+$  ratio for F15 is about 1.25, whereas it is about 1.4 for Fa3. We should point out that these results on kaons might be relatively rough since we do not consider any kaon-nucleon mean-field potential [35, 36, 37]. As far as we know, there is no explicit calculation about the difference of  $K^+$ - and  $K^0$ -nucleon potentials in the nuclear medium.

## V. SUMMARY

In this paper, we have investigated the role of the density-dependent symmetry potential in heavy ion collisions (HICs) at SIS energies, based on the UrQMD model (v1.3). The contribution of the Coulomb potential of mesons has been studied, in order to better understand the effects of the density-dependent symmetry potential on the dynamics of pions produced in neutron-rich HICs. The calculated results show a strong beam-energy dependence of the effect of the density-dependent symmetry potentials on the production ratios

$\Delta^-/\Delta^{++}$  as well as  $\pi^-/\pi^+$ . The uncertainty in the isospin-independent EoS alters the values of both the pion yields and the  $\pi^-/\pi^+$  ratios, but has almost no effect on the role of the density-dependent symmetry potential on the  $\pi^-/\pi^+$  ratios. The impact parameter is found to be important for the  $\pi^-/\pi^+$  ratios; for a larger impact parameter the effect of different density-dependent symmetry potentials on the  $\pi^-/\pi^+$  ratios becomes stronger.

The Coulomb potential of mesons changes the transverse momentum distribution of the  $\pi^-/\pi^+$  ratios significantly, though it leaves the total  $\pi^-$  and  $\pi^+$  yields almost unchanged. We find that the negatively charged pion yields, especially at midrapidity and low transverse momenta, as well as the  $\pi^-/\pi^+$  ratios at low transverse momenta, could be sensitive to the density-dependent symmetry potential in a dense nuclear matter. Quite a few pions are still produced at subnormal densities and thus are affected by the density-dependent symmetry potential at subnormal densities. These studies are of interest for forthcoming experiments at RIA (USA) and FAIR/GSI (Germany).

In this work, we have also investigated the yields of  $K^0$  and  $K^+$  mesons and the ratios  $K^0/K^+$  from neutron-rich HICs at  $E_b = 1.5A$  GeV. It is shown that they do not seem to be suitable to investigate the density dependence of the symmetry potential in dense nuclear matter. However, kaon production at energies much lower than threshold might improve the situation and is worth investigating further. Meanwhile, it is necessary to consider the difference of the  $K^+$ - and  $K^0$ -nucleon potentials in the nuclear medium.

### Acknowledgments

We would like to acknowledge valuable discussions with S. Schramm and A. Mishra. Q. Li thanks the Alexander von Humboldt-Stiftung for a fellowship. RK Gupta thanks Deutsche Forschungsgemeinschaft (DFG) for a Mercator Guest Professorship. This work is partly supported by the National Natural Science Foundation of China under Grant No. 10255030, by GSI, BMBF, DFG, and Volkswagen Stiftung.

---

[1] M. Prakash, I. Bombaci, M. Prakash, P. J. Ellis, J. M. Lattimer, and R. Knorren, Phys. Rep. **280**, 1 (1997).

- [2] J. M. Lattimer and M. Prakash, *Astrophys. J.* **550**, 426 (2001).
- [3] E. Chabanat, J. Meyer, P. Bonche, R. Schaeffer, and P. Haensel, *Nucl. Phys. A* **627**, 710 (1997).
- [4] B.-A. Li, *Phys. Rev. Lett.* **88**, 192701 (2002).
- [5] B.-A. Li, G.-C. Yong, and W. Zuo, *Phys. Rev. C* **71**, 014608 (2005).
- [6] T. Gaitanos, M. Di Toro, S. Typel, V. Baran, C. Fuchs, V. Greco, and H. H. Wolter, *Nucl. Phys. A* **732**, 24 (2004).
- [7] T. Gaitanos, M. Di Toro, G. Ferini, M. Colonna, and H. H. Wolter, nucl-th/0402041.
- [8] Q. Li and Z. Li, *Phys. Rev. C* **64**, 064612 (2001).
- [9] Q. Li, Z. Li, E. Zhao, and R.K. Gupta, *Phys. Rev. C* **71**, 054907 (2005).
- [10] J. Rizzo, M. Colonna, M. Di Toro, and V. Greco, *Nucl. Phys. A* **732**, 202 (2004).
- [11] Particle-Data Group, *Phys. Rev. D* **54**, 1 (1996).
- [12] Q. Li, Z. Li, and E. Zhao, *Phys. Rev. C* **69**, 017601 (2004).
- [13] A. Akmal and V.R. Pandharipande, *Phys. Rev. C* **56**, 2261 (1997).
- [14] H. Heiselberg and M. Hjorth-Jensen, *Phys. Rep.* **328**, 237 (2000).
- [15] B. A. Brown, *Phys. Rev. Lett.* **85**, 5296 (2000).
- [16] J. Margueron, J. Navarro, N. Van Giai, W. Jiang, nucl-th/0110026.

- [17] F. Hofmann, C.M. Keil, and H. Lenske, Phys. Rev. C **64**, 034314 (2001).
- [18] B. Liu, V. Greco, V. Baran, M. Colonna, and M. Di Toro, Phys. Rev. C **65**, 045201 (2002).
- [19] FOPI Collaboration, F. Rami *et al.*, Phys. Rev. Lett. **84**, 1120 (2000).
- [20] S. A. Bass *et al.*, Prog. Part. Nucl. Phys. **41**, 255 (1998).
- [21] M. Bleicher *et al.*, J. Phys. G: Nucl. Part. Phys. **25**, 1859 (1999).
- [22] H. Weber, E. L. Bratkovskaya, W. Cassing, and H. Stöcker, Phys. Rev. C **67**, 014904 (2003).
- [23] E.L. Bratkovskaya, M. Bleicher, M. Reiter, S. Soff, H. Stöcker, M. van Leeuwen, S.A. Bass, W. Cassing, Phys. Rev. C **69**, 054907 (2004).
- [24] I. Bombaci and U. Lombardo, Phys. Rev. C **44**, 1892 (1991).
- [25] D. Vretenar, T. Niksic, and P. Ring, Phys. Rev. C **68**, 024310 (2003).
- [26] D.T. Khoa and H.S. Than, nucl-th/0502059.
- [27] E.N.E. van Dalen, C. Fuchs, and A. Faessler, Nucl. Phys. A **744**, 227 (2004).
- [28] Q. Li, Z. Li *et al.*, Commun. Theor. Phys. **41**, 435 (2004).
- [29] A.M. Lane, Nucl. Phys. A **128**, 256 (1969).
- [30] J. Dabrowski, Phys. Rev. C **60**, 025205 (1999).
- [31] FOPI Collaboration, D. Pelte *et al.*, Z. Phys. A **357**, 215 (1997); *ibid* **359**, 55 (1997).

- [32] J. Y. Liu, Q. Zhao, S. J. Wang, W. Zuo and W. J. Guo, Nucl. Phys. A **687**, 475 (2001).
- [33] FOPI Collaboration, B. Hong *et al.*, nucl-ex/0501021.
- [34] Q. Li, Z. Li, S. Soff, M. Bleicher, and H. Stöcker, submitted to Phys. Rev. C (2005).
- [35] G. Q. Li, C. M. Ko, and B.-A. Li, Phys. Rev. Lett. **74**, 235 (1995).
- [36] C. Fuchs, A. Faessler, S. El-Basaouny, K. Shekhter, E. E. Zabrodin, and Y. M. Zheng, J. Phys. G: Nucl. Part. Phys. **28**, 1615 (2002).
- [37] M. Nekipelov *et al.*, Phys. Lett. B **540**, 207 (2002).

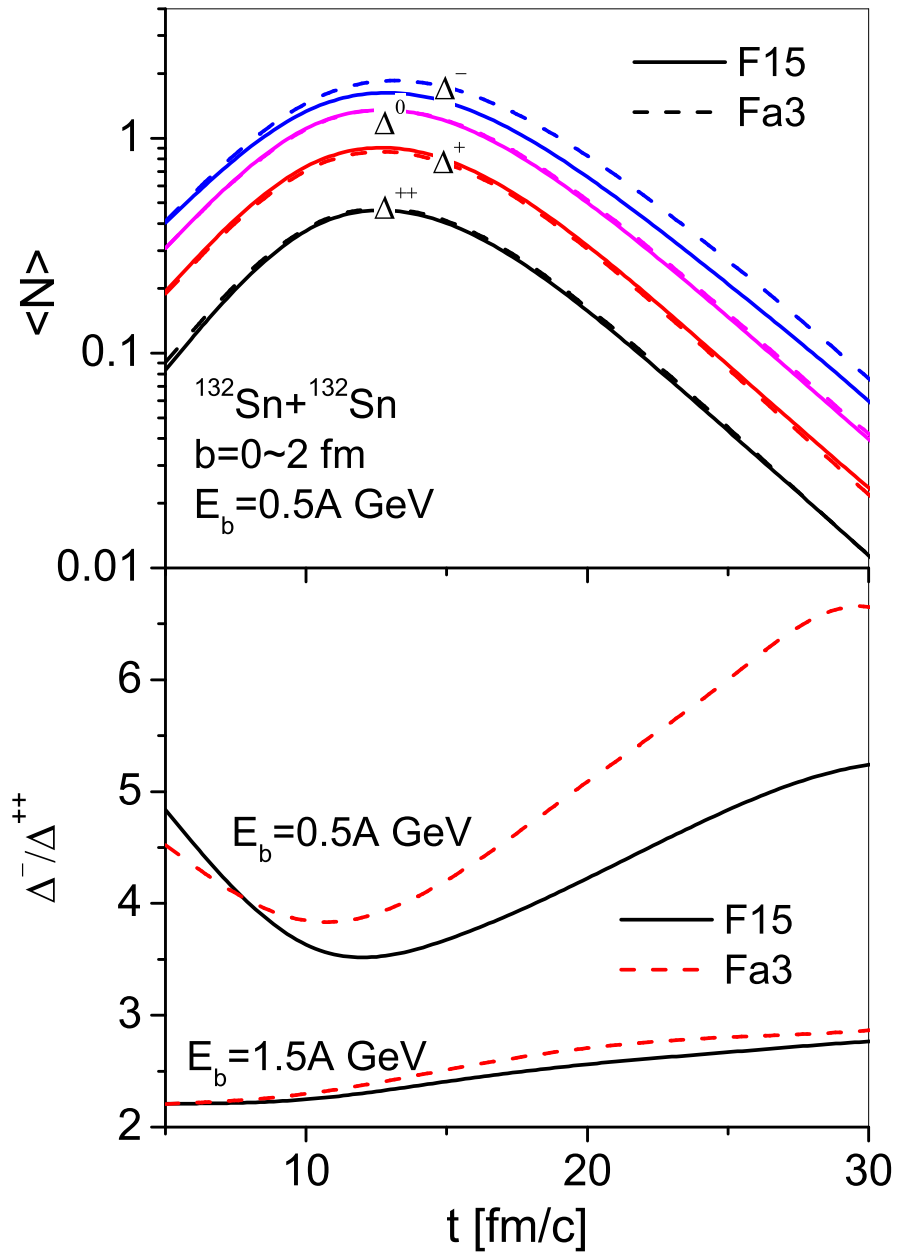


FIG. 4: Top: Time evolution of  $\Delta$  abundancies, for the symmetry potentials F15 and Fa3 at the beam energy  $E_b = 0.5A$  GeV. Bottom: Time evolution of the  $\Delta^-/\Delta^{++}$  ratio for the two symmetry potentials and at two beam energies  $E_b = 0.5A$  and  $1.5A$  GeV.

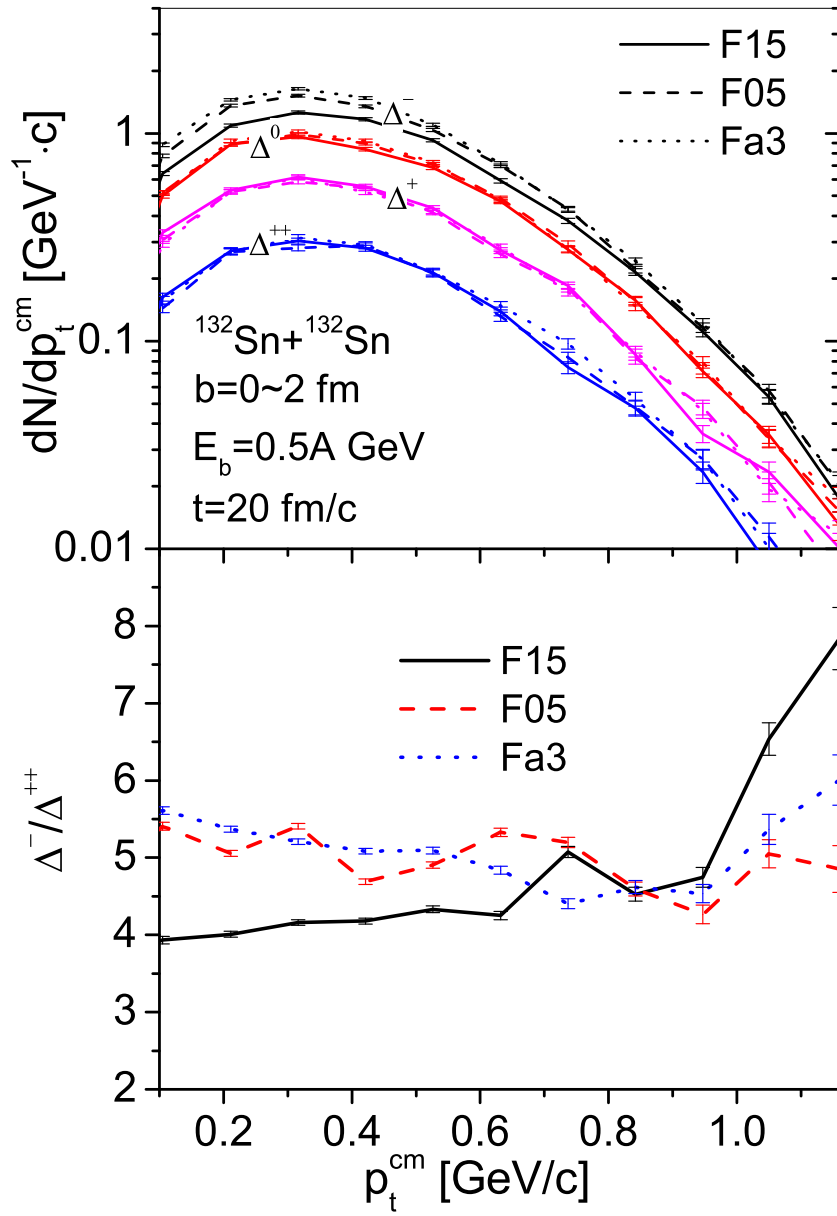


FIG. 5: Top: Transverse momentum distributions of various  $\Delta$  components for the symmetry potentials F15, F05, and Fa3, at  $E_b = 0.5A$  GeV, and  $t = 20 \text{ fm}/c$ . Bottom: The corresponding  $\Delta^-/\Delta^{++}$  ratios.

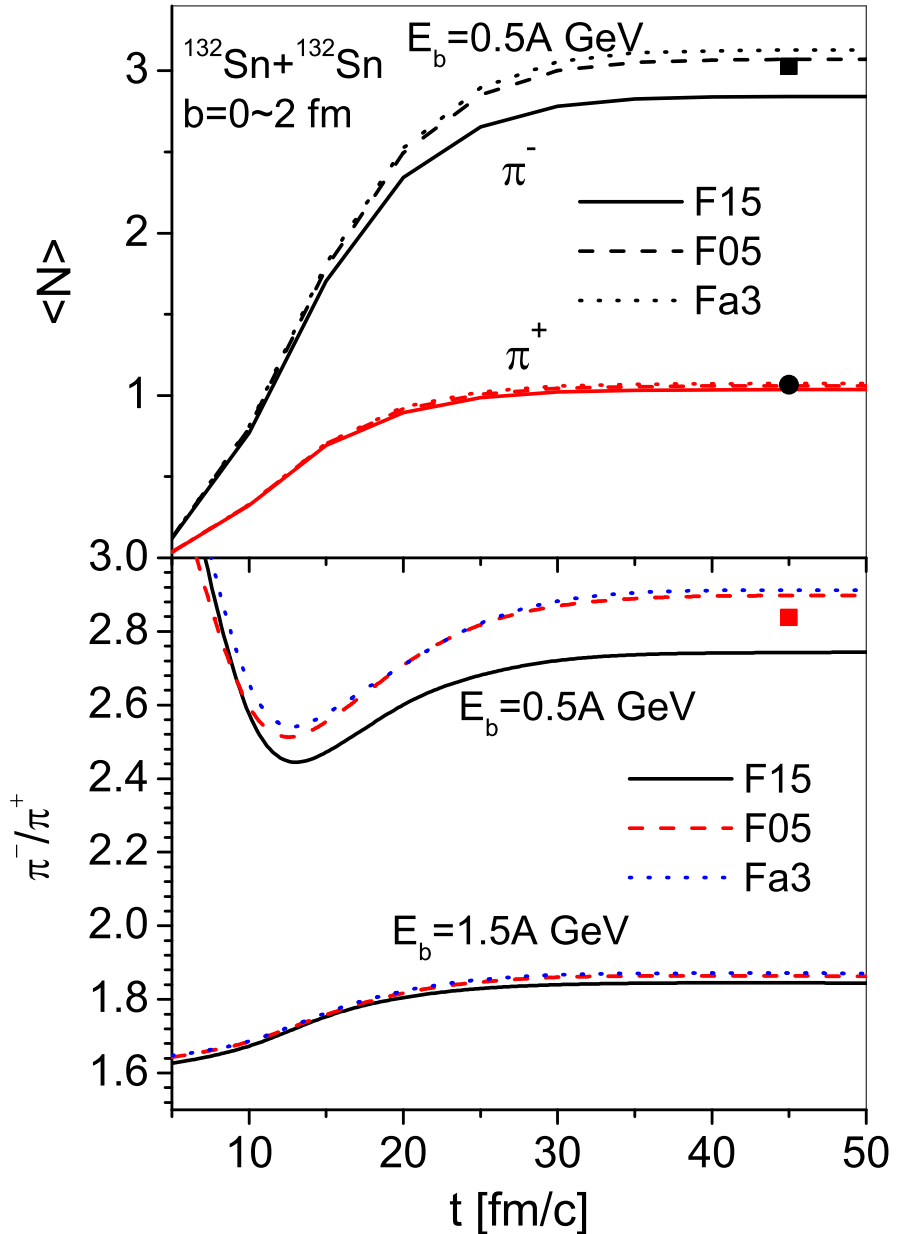


FIG. 6: Time evolution of the  $\pi$  abundances (top) and the  $\pi^-/\pi^+$  ratios (bottom) for the symmetry potentials F15, F05, and Fa3, at the beam energy  $E_b = 0.5A$  GeV. The Coulomb potential of mesons is switched off, except for the solid dots for the case F05 at  $E_b = 0.5A$  GeV. In the lower plot, the  $\pi^-/\pi^+$  ratio at  $E_b = 1.5A$  GeV is also shown.

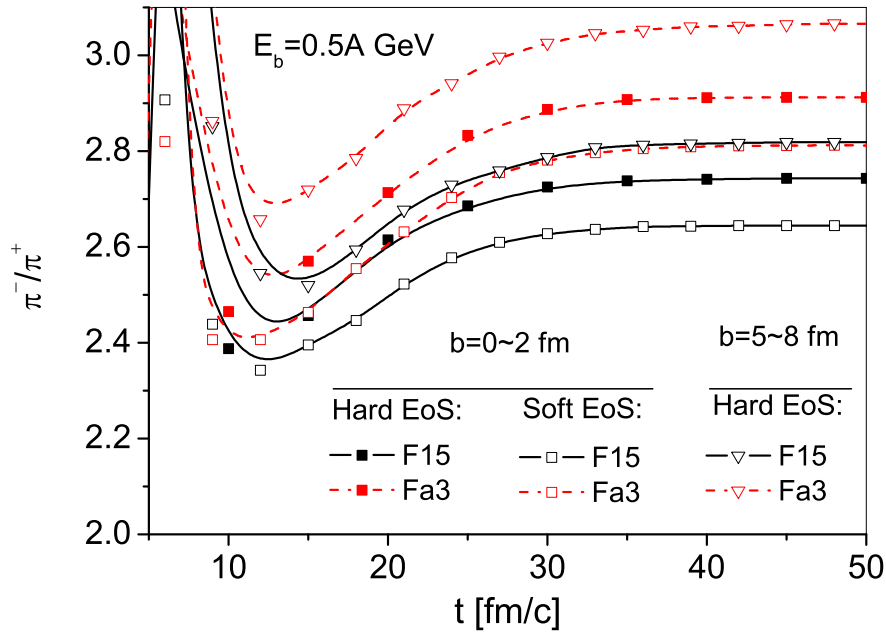


FIG. 7:  $\pi^-/\pi^+$  ratios from  $^{132}\text{Sn} + ^{132}\text{Sn}$  reactions at  $0.5A$  GeV, using a 'hard' and a 'soft' EoS with impact parameters  $b = 0 - 2$  fm and  $5 - 8$  fm. The symmetry potentials used are F15 and Fa3.

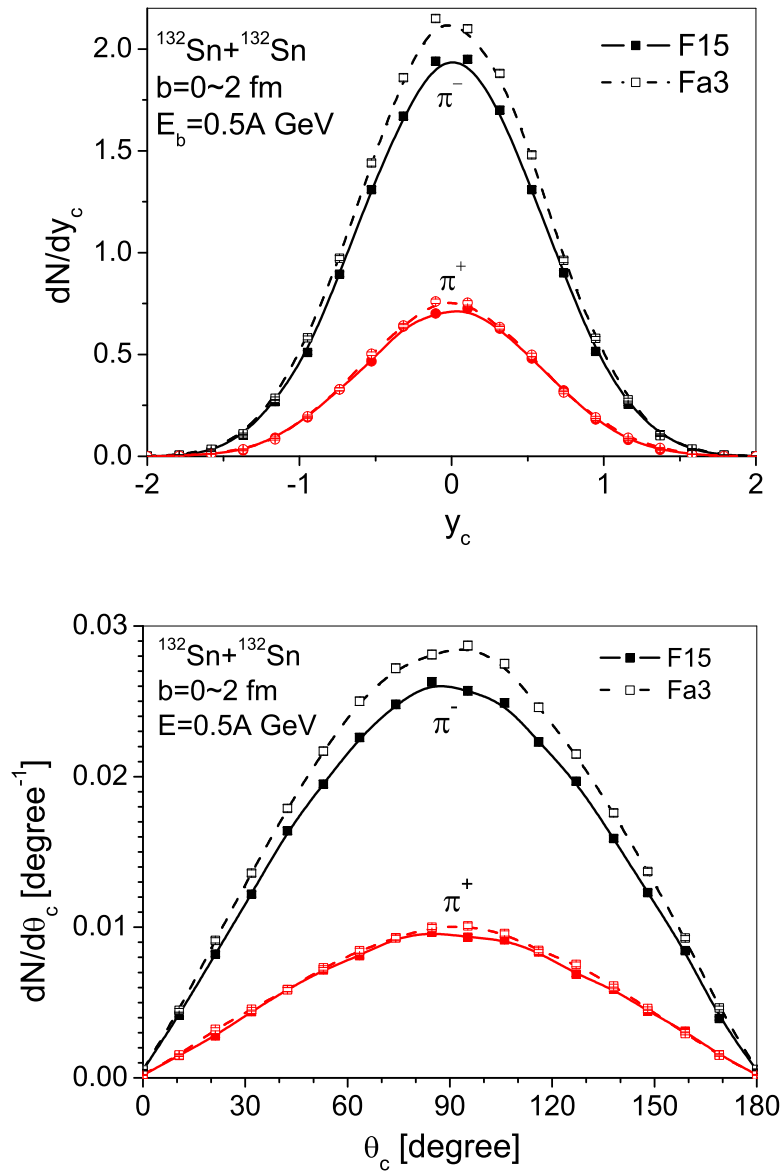


FIG. 8: Rapidity (top) and the polar angle (bottom) distributions of  $\pi^-$  and  $\pi^+$  in central  $^{132}\text{Sn} + ^{132}\text{Sn}$  collisions at  $E_b = 0.5A \text{ GeV}$ , for the symmetry potentials F15 and Fa3.

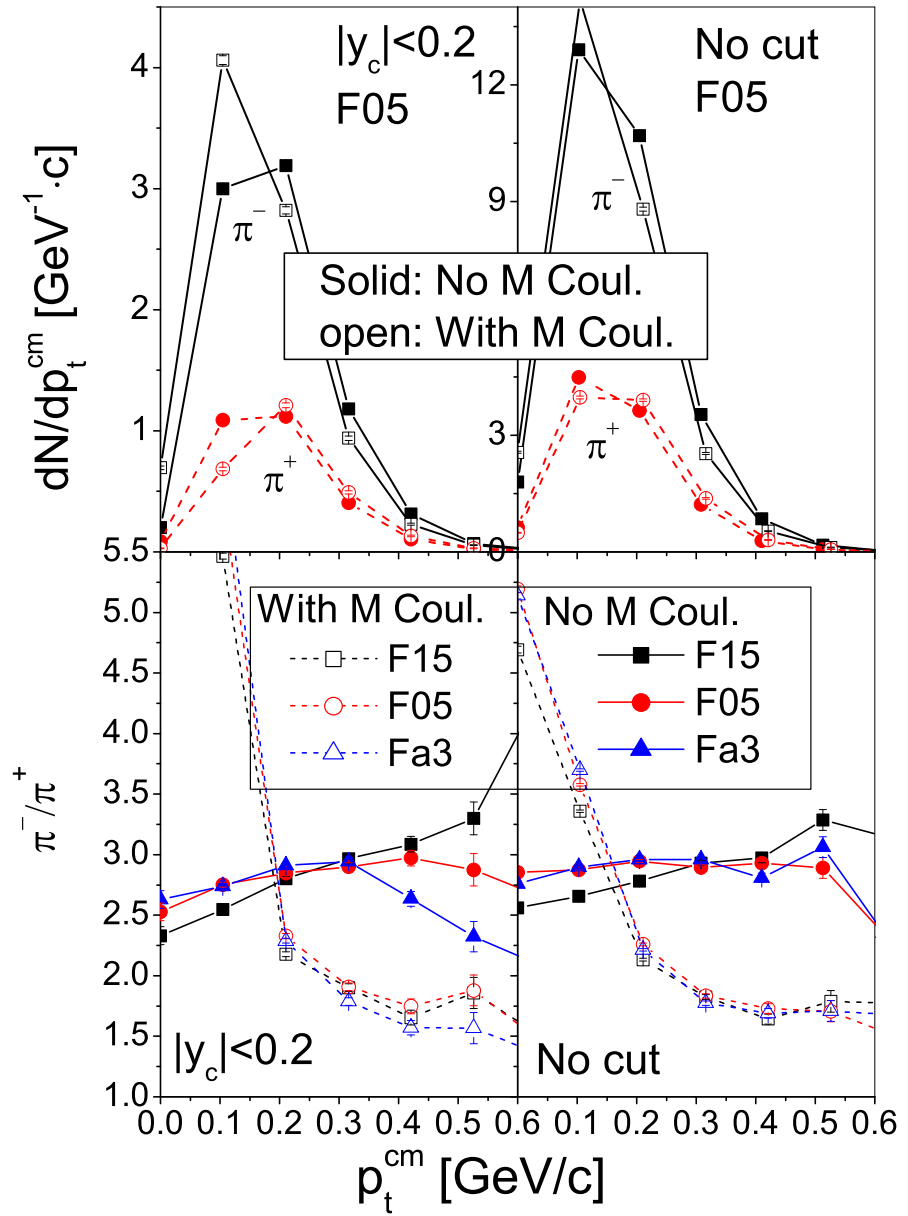


FIG. 9: Upper two plots: Transverse momentum distribution of  $\pi^-$  and  $\pi^+$  mesons with (left) and without (right) rapidity cut  $|y_c| < 0.2$ . The results with and without Coulomb potential of mesons (denoted as "M Coul.") are shown. The symmetry potential used is F05. Lower two plots: The corresponding  $\pi^- / \pi^+$  ratios, but for three different density-dependent symmetry potentials.

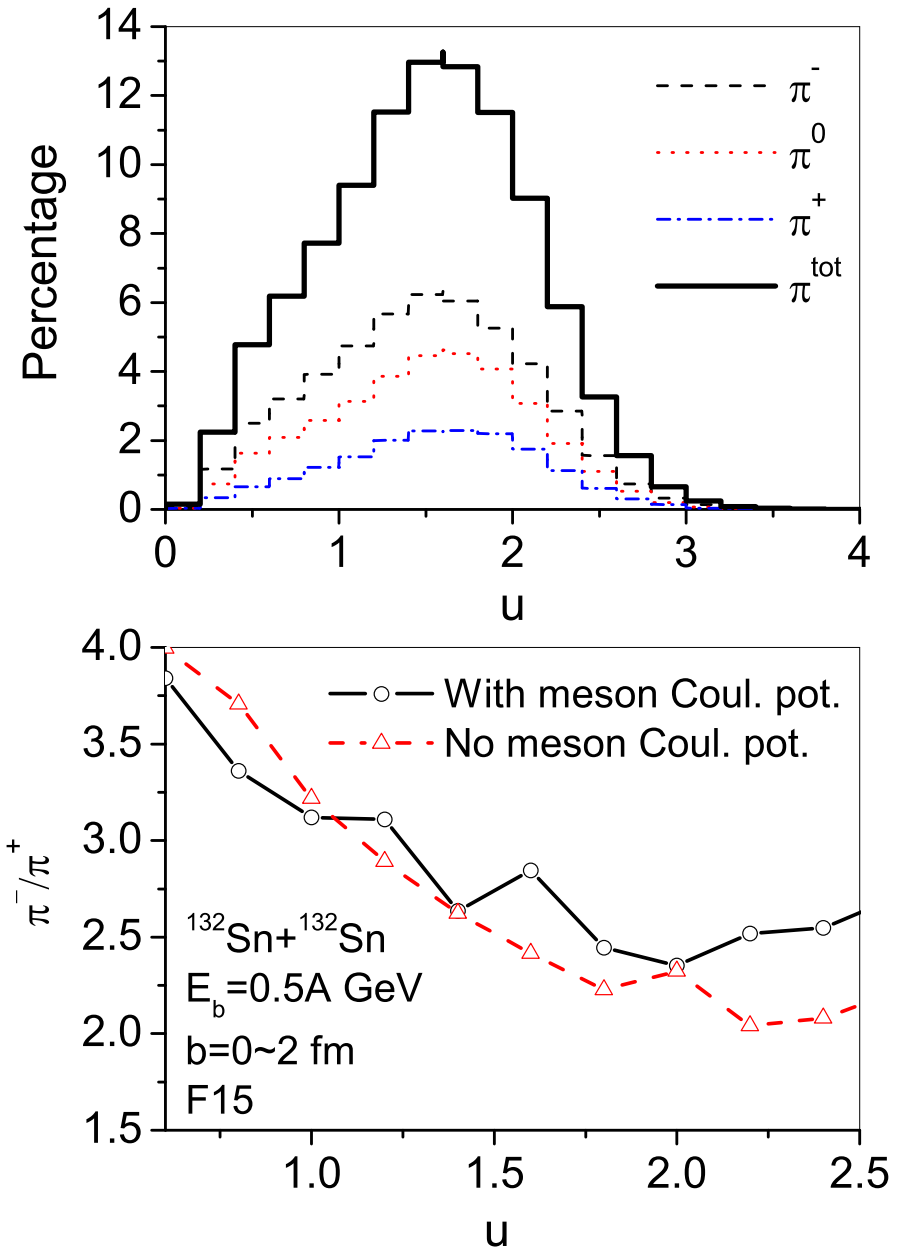


FIG. 10: Top: Percentages of the  $\pi$ 's as a function of reduced density, with the Coulomb potential of mesons included. Bottom: the corresponding density distribution of the  $\pi^-/\pi^+$  ratio of the percentages, with or without the Coulomb potential of mesons.

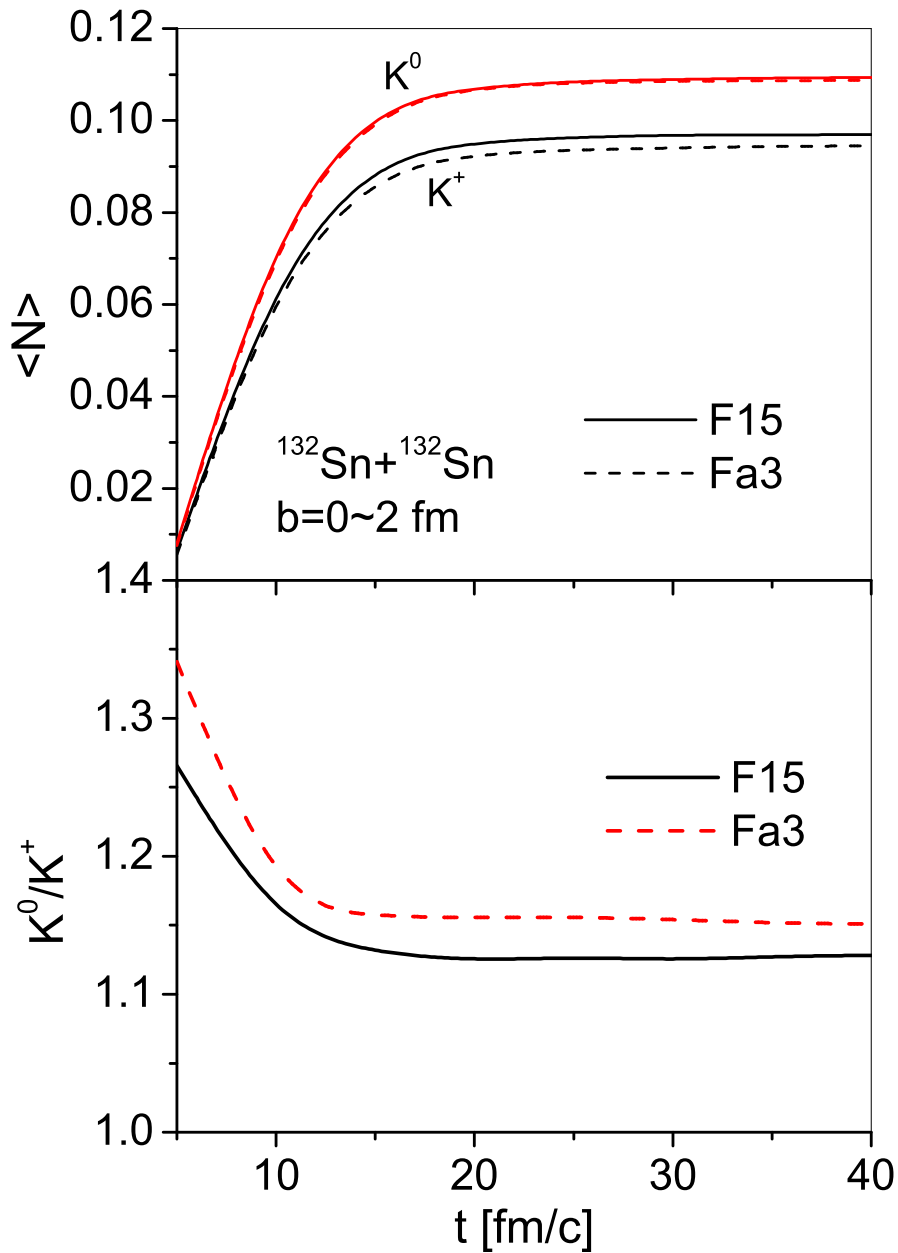


FIG. 11: Top: Time evolution of the  $K^0$  and  $K^+$  abundances for central  $^{132}\text{Sn} + ^{132}\text{Sn}$  collisions at a beam energy  $1.5A$  GeV and with the symmetry potentials F15 and Fa3. Bottom: the corresponding time evolution of the  $K^0/K^+$  ratios.